Electronic structure of a Co-decorated vicinal Cu(775) surface: High-resolution photoemission spectroscopy

S.-C. Wang,[1,*] M. B. Yilmaz,[1] K. R. Knox,[2] N. Zaki,[3] J. I. Dadap,[1] T. Valla,[4] P. D. Johnson,[4] and R. M. Osgood, Jr.[1,3]

[1]*Department of Applied Physics and Applied Mathematics, Columbia University, New York, New York 10027, USA*

[2]*Department of Physics, Columbia University, New York, New York 10027, USA*

[3]*Department of Electrical Engineering, Columbia University, New York, New York 10027, USA*

[4]*Department of Condensed Matter and Materials Science, Brookhaven National Laboratory, Upton, New York 11973, USA*

We measure the electronic structure of low-coverage Co on a Cu(775) stepped substrate using high-resolution photoemission spectroscopy with the particular goal of relating the electronic dispersion to the coverage-dependent surface structure. In particular, we follow the evolution of the electronic dispersion of the *sp*-like Cu surface state and the position of the band minimum as a function of Co coverage. On the bare Cu(775) surface, we observe band folding of this state due to the stepped surface-superlattice array. In addition, we determine that the reference plane, as measured by the position of the band minimum of this state, changes dramatically after addition of just 0.03 ML Co. At 0.06 ML, we observe the formation of a second surface state at a binding energy of 0.68 eV. This feature is attributed to a quantum-well state hybridized with the substrate.

PACS number(s): 73.22.−f, 73.20.At

INTRODUCTION

Recently, there has been an expansion of interest in understanding the physics of electrons on stepped metal surfaces. In part, this interest stems from the fact that, if carefully prepared, such surfaces can be used to examine electron physics at the nanoscale domain. Stepped arrays provide a "self-assembled" means of constructing a regular surface potential, which can either scatter or confine electrons in the lateral direction. Step arrays have provided insights into a variety of surface phenomena, including the formation of lateral superlattices, angular-asymmetric electron surface scattering, etc.[1–17]

While there have been a relatively large number of studies of electron behavior on bare stepped surfaces, the interest in bimetallic surfaces has only recently grown. Metal adsorbate-covered steps are of interest because the stepped substrate can, in principle, allow low-dimensional structures to self-assemble due to the selective growth at step edges or step risers.[18,19] An excellent example of such a system is Ag on Pt(997),[18] which has been demonstrated to exhibit row-by-row selective growth. Step-edge-defined magnetic nanowires have also been demonstrated, viz., the growth of Co nanowires on Pt(997).[19] Such epitaxial structures can enhance the lateral-confinement potential of surface electrons over that seen on bare surfaces. Even in cases where growth is more complex, exhibiting multilevel islanding, etc., the presence of steps can alter growth and, hence, allow new nanostructures to form. For example, a regular stepped surface can act to increase the nucleation density for low-coverage adsorbate atoms and the higher nucleation density can lead in turn to the self-assembly of a high density of nanoscale islands. Copper stepped surfaces have provided some of the more important surfaces for the study of surface nanoelectronic structure, as well as step-step interactions. Because of this, stepped Cu is an appropriate choice for the study of bimetallic surface structures and, in fact, there have been recent studies[1,3] of, for example, Ag on vicinal Cu sur-

faces. Further, such exploration represents a natural extension of earlier studies of Co grown on flat Cu surfaces, particularly Cu(111). Here the interest is in the possible use of such structures in magnetic spin valves.[20–30] Surprisingly, there has been to date, limited work on the growth of Co on stepped Cu(111).[22–24] In this paper, we make use of Co/Cu(775) system to examine the associated surface nanostructures and their electronic structure.

The Cu(775) surface (see Fig. 1) is formed from an 8.5° vicinal cut of Cu(111) along the [11$\bar{2}$] direction. At the center of the zone, the bare Cu(111) surface has a projected bulk band gap extending from 0.9 eV below the Fermi level, E_F, to 4.1 eV above. An *sp*-like surface state existing within this gap has a band minimum at 0.43 and 0.39 eV below E_F at 30 K and room temperature, respectively,[31,8] and a parabolic dispersion with an effective mass, m^*, of approximately $0.41m_e$ where m_e is the free electron mass. When cut into the vicinal Cu(775) surface, the 14.3-Å-wide (111) terraces are separated by monatomic steps. Such stepped surfaces are known to self-assemble into relatively monodispersed terrace-row-number arrays. In the case of Cu(775) at 300 K, the distribution of terrace widths is approximately a Poisson distribution with a standard deviation of ±1 atomic row.[5]

On a bare, *vicinal* Cu(111) surface, the electronic structure is known to change from that on the Cu(111) surface due
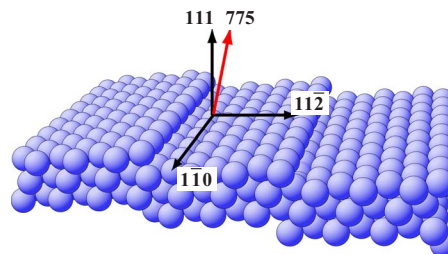

FIG. 1. (Color online) Sketch of well ordered Cu(775); the terrace width is 14.3 Å and the sample cut is such that the step descends along the [11$\bar{2}$] direction.

115448-1

to the interplay of several effects. For example, the step-induced dipoles that form change the local work function from that of the flat surface. Electron confinement to the step terraces causes the band minimum of the *sp*-surface state to shift upward while the terrace-width distribution and the reduced photohole lifetime broadens the bandwidth.[1] In addition, several studies of both occupied and unoccupied states on different vicinal surfaces have shown that band folding will result from umklapp scattering from the superlattice defined by the periodic steps. The importance of the periodic surface potential has been correlated with the average terrace width.[1–7,13] This has been observed, for example, on Cu(775) using angle-resolved measurements of image states with two-photon photoemission (2PPE) spectroscopy.[5] Umklapp processes have also been observed for adsorbate-covered vicinal surfaces.[1]

In the case of bimetallic systems, studies have been more limited. A study of Ag on vicinal Cu found that the deposition of Ag substantially changed the step structure from that of the bare surface.[3] In addition, studies of the electronic structure showed evidence of a change from two-dimensional to one-dimensional dispersion with increasing Ag coverage, as well as evidence of two distinct compositionally controlled surface states.

Because of the interest in layered magnetic structures, there have also been extensive measurements of the growth and electronic structure of Co on Cu(111) using scanning tunneling microscopy (STM), photoemission, and inverse photoemission.[20–28,32] In contrast to growth on Cu(100) where the Co adsorbate structure grows in a nearly ideal layer-by-layer mode,[33] STM studies of Co grown on Cu(111) have shown that the initial growth occurs via bilayer islands with evidence of subsurface Co insertion.[20,24,25,32] The Co islands are triangularly shaped and oriented at 60° with respect to each other. A recent STM study showed that at low coverage, bilayer growth of Co proceeded preferentially along the upper step edges,[24] an effect which was ascribed to an ~1 eV Ehrlich-Schwoebel barrier for movement of Co to the lower terrace level. More complex multilayer island growth was observed at higher coverage. In addition, Co deposition can lead to more complex surface restructuring, including spontaneous etching and mass transport at low coverage.[23,24] Co, Fe, and W adsorption on stepped Cu surfaces has been the subject of a recent theoretical investigation.[34] This study suggests the stabilization of a row of adsorbate atoms along the upper edge of the step with activation energies of the order of 1 eV. This structure will prevent the adsorbates from "hopping" down the step edge.

The electronic structure of the Co/Cu(111) system has also been examined previously. Several groups have made measurements of this structure on Co deposited on single-crystal Cu(111). Much of the work focused on determining the spin-exchange splitting of this bimetallic system and included photoemission spectroscopy,[26,27] inverse photoemission,[28] and theoretical calculations.[30] These were followed by studies of the effects of vicinal surfaces on this electronic structure. For example, angle-resolved photoemission spectroscopy (ARPES) measurements were made of the electronic structure of Co nanoclusters on Cu(755).[29] At low coverage, the Co states displayed a nearly flat isotropic dispersion and the *d*-band lower minority and majority states shifted with coverage. The authors noted that both of these observations were consistent with the formation of Co nanoclusters.

In the present paper, we report a study of the coverage-dependent electronic structure of vicinal Cu(111), in particular, Cu(775) in the presence of low-coverage Co adsorbate. As discussed above, earlier work has focused on changes in the Co electronic structure with coverage. Because of the focus on the Co overlayer, these studies employed either *s*-polarized light or high-energy photons to suppress the strong Cu surface-state peak. In the present work, by making use of *p*-polarized light, we describe an investigation of the changes in both Co and Cu features, including the Cu surface state. Our results at low cobalt coverage reveal several striking step-lattice-related phenomena. In particular, we observe bare-Cu-surface step-array band folding and, after addition of a fraction of a monolayer of Co, we also observe a shift in the position of the band minimum of the Cu surface state and the formation of a new surface state at a higher binding energy. The origin of these features is discussed in the context of prior work on step surfaces.

EXPERIMENT

Angle-resolved photoemission measurements were carried out on the undulator beamline U13UB at the National Synchrotron Light Source at Brookhaven National Laboratory, equipped with a Scienta SES2002 analyzer. UV *p*-polarized light, with photon energies ranging from 16 to 25 eV, was focused to a spot $<100 \mu$m in diameter on the sample in an UHV chamber with pressure less than 1 $\times 10^{-10}$ Torr. The energy resolution of the beamline and the analyzer was ~10 meV and the angular resolution of the detector was $<0.2°$, corresponding to a momentum resolution of 0.008 Å^{-1} at 25 eV photon energy.

The Cu(775) crystal was prepared by repeated Ar$^+$ sputtering at room temperature and annealing to 500 °C until sharp split spots were observed with low-energy electron diffraction, indicating high step regularity. Step regularity could also be determined via the photoemission spectra, since these measurements showed umklapp bands (see below) when a regular stepped surface was formed. The Co source was an e-beam-heated Co rod. The chamber pressure remained at less than 5×10^{-10} Torr during Co deposition. The deposition rate was monitored using a quartz-crystal thickness monitor. All data were recorded at room temperature.

EXPERIMENTAL RESULTS

Measurements and results for clean Cu(775). Prior to any deposition of Co, the clean Cu vicinal surface already displayed features originating from its nanostructured surface. For example, Fig. 2 shows data taken at 25 eV photon energy from the clean Cu(775) surface. The spectra were recorded in a direction perpendicular to the step edges. Dispersion curves determined from the raw data are indicated with solid lines. In fitting the energy-distribution curves (EDCs) for each parallel momentum value, the raw data are angle
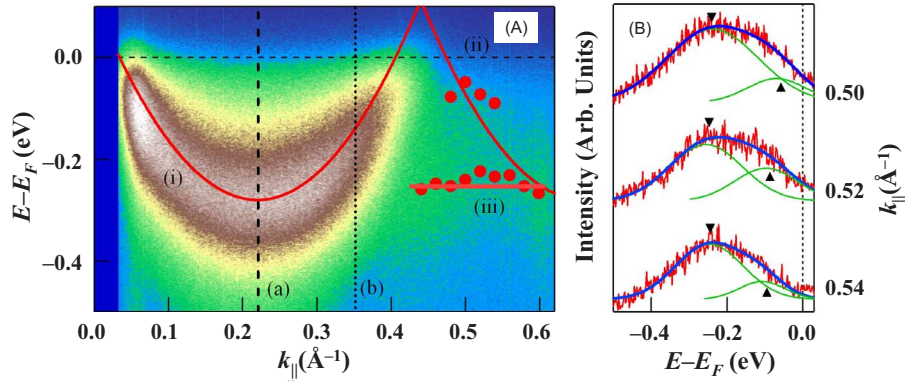
FIG. 2. (Color online) (A) The measured bare Cu(775) surface-state dispersion using 25 eV photon energy. Note that the main band is centered on the surface Brillouin-zone boundary of the superlattice, designated by the dashed line (a). The parallel momentum corresponding to the terrace-normal direction is indicated by the dotted line (b). The parabolic continuous curve labeled (i) is a quadratic fit to the main band. The second continuous curve (ii) is a 0.44 Å^{-1} ($2\pi/d$)-shifted replica of the fit. The curve indicated by (iii) is a weak- to nondispersive state, typical of many stepped surfaces. (B) An example of peak fitting the weak features to the right of the main band. After an appropriate background subtraction a sum of two Gaussian curves was used to fit the data. Three energy-distribution curves are shown at the parallel momenta indicated on the right. The downward- and upward-facing arrows indicate the nondispersive state and the umklapp band, respectively.

integrated about an angular interval of 0.6° to increase the signal-to-noise ratio and a Gaussian line shape is used to fit the peaks [see Fig. 2(b)]. In brief, the figure shows the usual Cu surface state and its dispersive behavior, but with a decrease in binding energy relative to that of the flat Cu(111) surface. In addition, there is evidence of umklapp or band folding due to the presence of the periodic step array. The dispersion curve centered at the surface-superlattice Brillouin-zone (SSBZ) boundary is obtained by a least-square fit to the peak positions of the angle-resolved data up to 0.4 Å^{-1}. In the region to the right of the main band, the peak positions for a nondispersing state and the folded band, as determined by peak fitting, are indicated with filled circles.

The bottom of the main band at $k_{\parallel}=0.22$ Å^{-1} is ~280 meV below the Fermi level. This position is ΔE ~110 meV higher than the minimum of the clean Cu(111) surface state at room temperature.[8] In addition, the peak is broader (full width at half maximum $\Delta\Gamma \sim 200$ meV) than the same feature from a well prepared Cu(111) surface.[35] These changes in the binding energy and the linewidth, ΔE and $\Delta\Gamma$, are consistent with a linear relationship between the two as observed previously on other vicinal copper surfaces.[1] Several STM and photoemission measurements have previously observed shifts in binding energy on vicinal surfaces due to the terrace confinement by the step potential.[1,2,6–8] The exact magnitude of the binding-energy shift and the linewidth broadening depends on the angle of the vicinal cut;[1] binding-energy shifts as high as ~250 meV, and linewidth broadening as large as 400 meV have been observed.[8]

The shift in binding energy can be placed on a more quantitative footing by using a Kronig-Penney model for the step potential. Modeling the steps as a series of delta functions with amplitude V_0 separated by a distance b, we obtain the energy-momentum relationship

$$\cos(kb) - \cos(qb) - \frac{mV_0}{\hbar^2 q}\sin(qb) = 0, \tag{1}$$

where the energy associated with scattering from the steps, E_S, is given by $E_S = \hbar^2 q^2/2m$. Near the minimum of a parabolic band, k and q are sufficiently small so that Eq. (1) can be manipulated to yield

$$\tan\left(\frac{qb}{2}\right) = \frac{qb}{2} = \frac{mV_0}{\hbar^2 q}, \tag{2}$$

from which it follows that

$$E_S(b) = \frac{V_0}{b}. \tag{3}$$

This shift is a small perturbation on the clean surface-state energy such that the measured energy $E_{min}(b) \approx E_{min}(111) - E_S(b)$. As shown in Fig. 3, plotting $E_S(b) = E_{min}(111)$
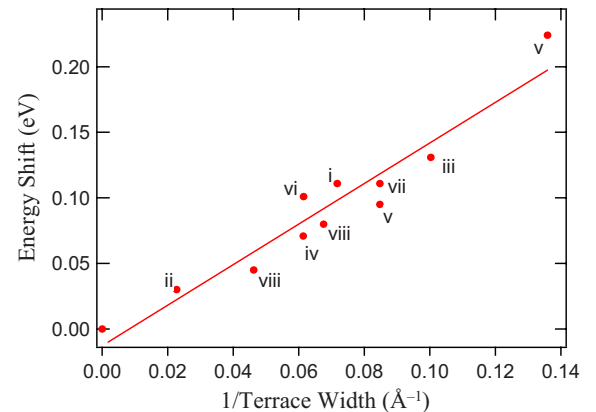

FIG. 3. (Color online) Shift of the band minimum versus inverse terrace width. Data are collected from (i) this work and Refs. (ii) 1, (iii) 3, (iv) 6, (v) 8, (vi) 9, (vii) 10, and (viii) 11.

$-E_{min}(b)$ against $1/b$ therefore gives a measure of V_0. The data in Fig. 3 are taken from the present work and from studies of other vicinal surfaces.[1,3,6,8–11] The gradient gives $V_0 = 1.55$ eV Å, which compares closely with the value of 1.25 eV Å found in an STM study of Sánchez *et al.*[11]

As discussed above, prior work has also considered the surface-state linewidths on vicinal surfaces.[1,6] In particular, in Ref. 1, a linear relation between the change in linewidth and binding-energy shift was found for a series of vicinal surfaces; the dominant contribution to this variation was ascribed to photohole lifetimes, which are known to be dependent on scattering processes at the steps. A second contribution to the linewidth is the terrace-width distribution (TWD), which can be modeled using the Kronig-Penney model described above and assuming a Gaussian distribution of terrace widths.[6] This TWD is found to account for less than 30% of the change in linewidth.[1] Our data show a linewidth broadening of 200 meV, a value in close agreement with the value based on the linear relation given in Ref. 1.

Considering the step-induced changes in the spectrum in more detail, we note that, as shown in Fig. 2, the *sp*-band minimum is centered away from either the surface normal (defined by the [775] direction) or the terrace normal (defined by the [111] direction). Upon closer inspection, this position can be identified as the SSBZ boundary, which is 0.22 Å^{-1} away from the zone center for Cu(775). Prior studies using ARPES have also observed a variation in the position of the band minimum as the vicinal-cut angle is changed.[1–3,5–10,12,13] In these earlier studies, a reference plane identical to the overall surface plane is generally seen for vicinal cuts larger than 5°; such an observation is termed "surface modulated."[12] On the other hand for miscut angles smaller than 5°, the reference plane is that of the local terrace plane; such an observation is termed "terrace modulated," where the terrace represents the (111) plane. These observations are in accord with the present study where with the surface cut at 8.5°, the position of the band minimum occurs at the SSBZ boundary, which is consistent with *surface* modulation of the *sp* state rather than *terrace* modulation. Such surface-modulated electron wave functions extend over several terraces and exhibit free-electron-like dispersion in the average surface (775) plane as opposed to the terrace plane. In the case of terrace modulation, the electron wave function across the steps is localized on individual terraces with a band minimum centered at the terrace normal.

Near the minimum of the band, the Cu(775) surface state displays parabolic dispersion, with an effective mass of $\sim 0.47 m_e$. In the vicinity of the Fermi level at $k_\parallel \sim 0.2$ Å^{-1} away from the band minimum, using greater data magnification we find that the band dispersion turns negative. Note that these data points shown were obtained by peak fitting with two Gaussian peaks as shown in Fig. 2(b). We attribute this behavior to band folding due to the step-array superlattice along the [11$\bar{2}$] direction. The solid line showing the folded band in Fig. 2 is obtained by shifting the original band by 0.44 Å^{-1}, which corresponds to a terrace width of $d \sim 14.3$ Å. The data points around the expected folded band position show significant scatter because at the normal wave vector corresponding to the 25 eV photon energy, the inten-
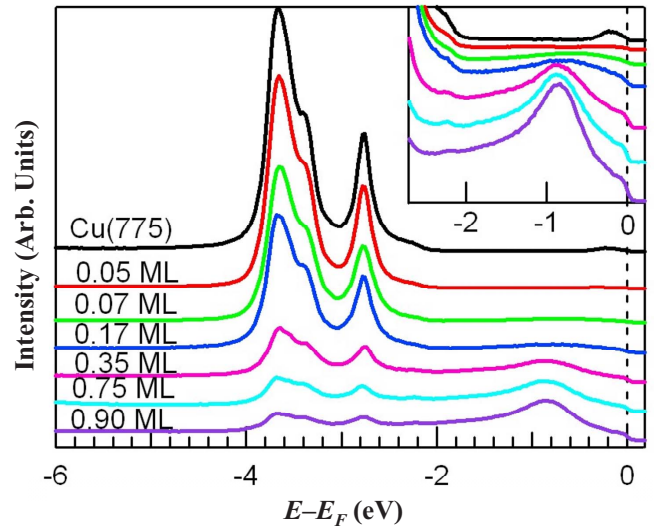

FIG. 4. (Color online) Evolution of EDCs as a function of Co coverage at $k_\parallel = 0.22$ Å^{-1}. The inset to the figure shows features close to the Fermi level in greater detail for the same sequence in Co coverage as in the main figure. Experiments are performed using 25 eV incident photon energy.

sity of umklapp band is known to be weak.[2,13] The relatively weak emission from the umklapp feature seen here is consistent with results obtained in earlier photoemission measurements on vicinal Cu and Au surfaces.[13,14]

An additional feature of the bare Cu(775) surface band structure in Fig. 2 is the faint but persistent nondispersive state located at ~ 250 meV below the Fermi level. Similar features have been reported in other ARPES and 2PPE experiments.[15–17,36,37] The observation has been variously attributed to terrace confinement,[2] to a one-dimensional state formed by step edges,[15] or to disorder localization due to nonuniformity in terrace widths.[37]

Measurements and results for low-coverage Co on Cu(775). An important component of the present work is the study of the effect of low-coverage Co on the electronic structure of the stepped Cu surface. Our results show that Co induces changes in the Cu surface state reference plane as well as new states. Co was deposited on the Cu(775) surface to various coverages ranging from a fraction of a monolayer to almost a full monolayer. Figure 4 shows the photoemission spectra recorded at $k_\parallel = 0.22$ Å^{-1} as a function of coverage. As the Co coverage is increased, the Co 3*d*-band emission at around 0.8 eV binding energy increases and the intensities of the multiple Cu 3*d* peaks (with binding energies between 2 and 4 eV) decrease. Note that the Cu 3*d* peaks are still visible even at the highest coverage of 0.9 ML due to the island-growth mode (see below) for Co on Cu(111).

Earlier studies of Co on Cu (Refs. 26–29) had focused almost exclusively on changes in the electronic structure of the adsorbed-Co phase. In contrast, the evolution of Cu states and, in particular, the Cu surface state was not studied in detail. These changes form the core of the present study. Clearly, the Cu surface-state signal is lost completely for the higher Co coverage. However, at low coverages, less drastic
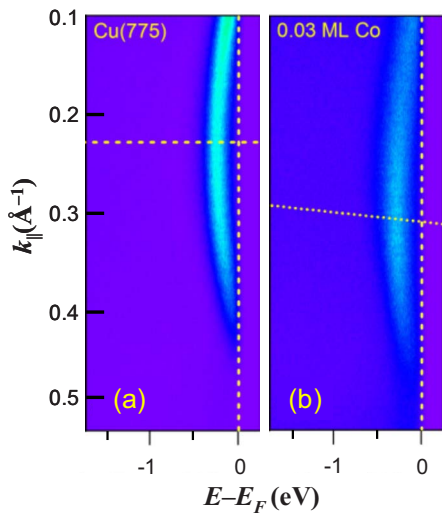
FIG. 5. (Color online) Angle-resolved photoemission from (a) clean Cu(775), and (b) 0.03 ML Co-covered surface at 21 eV incident photon energy. On clean Cu, the surface state is centered at the surface-superlattice Brillouin-zone (SSBZ) boundary, i.e., $k_\parallel$ =0.22 Å^{-1}. Upon cobalt deposition, the band shifts to a position close to terrace normal at $k_\parallel$=0.31 Å^{-1}. Note that the parallel momentum corresponding to the terrace-normal direction [the dotted line in (b)] is a function of binding energy since the (111) terraces are oriented at a fixed angle (8.5°) with respect to the (775) surface.

but nonetheless important changes in the Cu surface state are also readily observed. A particularly striking example is a change of the reference plane of the Cu surface state, which is defined by the (775) plane for the clean surface. Figure 5 shows a comparison of the 21 eV angle-resolved ultraviolet photoemission spectroscopy measurement of the surface state before and after deposition of 0.03 ML of cobalt. Before the Co deposition, the dispersion minimum is clearly located at $k_\parallel$=0.22±0.02 Å^{-1}. After deposition of 0.03 ML of Co, the minimum changes position to $k_\parallel$ =0.31±0.02 Å^{-1}. An examination of the surface structure for Cu(775) shows that these minima correspond to a shift in the band minimum from the SSBZ boundary to, within experimental error, that of the terrace normal. This observation is probably a reflection of the fact that the initial deposition "roughens" the step edges, thereby decreasing the Fourier component associated with the step structure from the surface-electron scattering potential.

Other changes can be observed at slightly higher cobalt coverages. In particular, Fig. 6 shows data taken at Co coverage of 0.06 ML with 25 eV photon energy; representative EDCs corresponding to the SSBZ ($k_\parallel \approx 0.22$ Å^{-1}) and terrace normal ($k_\parallel \approx 0.34$ Å^{-1}) are shown in the figure. In order to improve upon signal to noise ratio, the experimental data are angle integrated over an interval of 0.6° about each data point and least-square fit with Gaussian line shapes. This process enabled us to obtain the data fit shown in Fig. 6. The data shown in Fig. 6 show a new dispersive band with higher binding energy (E_B=0.68 eV) and centered at the SSBZ boundary. In general this feature which is first observed at ~0.04 ML Co-covered surface is seen to increase with Co coverage peaking at ~0.06 ML before slowly decreasing
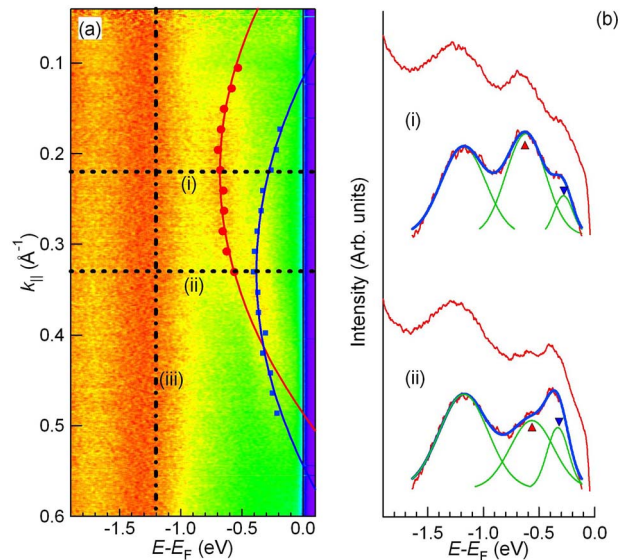

FIG. 6. (Color online) (a) Angle-resolved photoemission from 0.06 ML Co-covered Cu(775) taken at a photon energy of 25 eV. The nondispersive feature labeled (iii) at ~1.2 eV binding energy is due to emission from Co. In addition to the shifted Cu(775) surface state (blue squares), a new state with 0.68 eV binding energy appears at the SSBZ boundary (red dots). (b) EDCs taken at parallel momenta corresponding to (i) the SSBZ boundary and (ii) the terrace normal are shown along with Gaussian fits to the background subtracted EDCs. The shifted Cu(775) surface state is indicated by a downward-facing blue arrow and the new state by an upward-facing red arrow.

with the addition of more Co. The residue of the original Cu surface state, which had shifted to terrace modulation after adding 0.03 ML of Co to the bare Cu surface, can still be seen at this higher coverage. Since the 25 eV incident photon energy of Fig. 6 is higher than the 21 eV in Fig. 5 and the electrons are emitted in the fixed, terrace-normal direction, i.e., 8.5° off the surface normal, the band minimum appears at $k_\parallel$=0.34±0.02 Å^{-1} as opposed to $k_\parallel$=0.31±0.02 Å^{-1} in Fig. 5. This is another evidence for the terrace-modulated nature of the observed band. Another broader feature is apparent at ~1.3 eV. Experiments performed as a function of Co coverage show that this broader peak smoothly shifts toward the position of the Co d band in bulklike thin films and can thus be attributed to a cobalt d-band state.[26,27,38] It would be interesting to know whether this feature is nondispersive along the steps. However, data at 0.06 ML were not collected due to time constraints at the beamline. Note however, that several related observations can be made. Although not shown here, ARPES data were measured at higher coverage, which showed weak dispersion of the 3d-band state as expected. Finally, the presence of a nondispersive state appears to confirm the island growth of the cobalt and in the earlier work performed on Co/Cu(755) by Ogawa et al.,[29] the 3d band was observed to be nondispersive both along and across the steps.

Returning now to the 0.68 eV feature centered at $k_\parallel$ =0.22 Å^{-1} we note that it resembles the states observed in earlier studies of lateral quantum-well structures on stepped
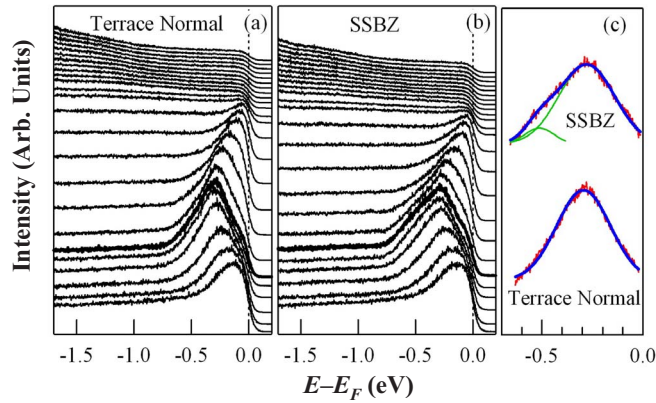
FIG. 7. (Color online) Angle-resolved photoemission measurements along the steps (y direction, see text), taken at a 1° interval from 0.04 ML Co-covered Cu (775). The top and bottom curves correspond to 19° and −5°, respectively. ARPES data at (a) k_x ~ 0.34 Å^{-1} (terrace normal) and (b) k_x=0.22 Å^{-1} (the SSBZ boundary) in the direction across the steps; (c) comparison of EDCs for the two cases at k_y=0 Å^{-1} along with Gaussian fits to the background subtracted EDCs.

surfaces.[3,7] The state shows considerable dispersion having an effective mass of ~$0.4m_e$. This observation is consistent with earlier studies that concluded that at low coverage the dispersion of a quantum-well state reflects hybridization with the substrate.[39] As such, the dispersion of the state will be determined by the dispersion rate of the bottom of the bulk band gap along the (111) direction. Indeed all states at low coverage on this system should show a similar dispersion, as is observed. The band centered at $k_\parallel$=0.34 Å^{-1} yields $0.46m_e$, essentially identical to that of the bare Cu(775) surface state. Finally note that alternative explanations of the origin of this state are possible, e.g., modification of the step-edge potential due to adsorption of Co.[40] A more complete resolution of the physics of this state would be an interesting subject of additional experiments.

Figure 7 shows ARPES data taken for angular variation parallel to the steps following the deposition of 0.04 ML Co. The data are taken at an incident photon energy of 21 eV, and by rotation of the sample around an axis perpendicular to both the terrace normal and the step edges. The angular data interval along the steps is 1°, that is, each EDC curve has a 1° separation along the steps; these measurements are taken from −5° to 19°. In addition to improve the signal to noise ratio, each of these same EDCs is also integrated about an angular interval of 2° perpendicular to the steps. If we define k_x and k_y as parallel momenta across and along the steps, respectively, panels (a) and (b) show data at two values of k_x: one for emission normal to the terraces (k_x ~ 0.34 Å^{-1}) and one corresponding to the SSBZ boundary (k_x=0.22 Å^{-1}). At this relatively low Co coverage and for this photon energy, the Co d bands are not yet visible. However, the effect of Co deposition can be clearly seen by plotting the EDCs at the band minima (i.e., at k_y=0 Å^{-1}) of Figs. 7(a) and 7(b), corresponding to the terrace normal and SSBZ, respectively. In particular, we observe that at the minimum of the band (k_y=0 Å^{-1}), the SSBZ EDC is slightly more distorted than the terrace-normal EDC as shown in Fig. 7(c). As is shown by

the curve fitting in Fig. 7(c), this broader feature of the SSBZ curve arises from the overlap of two states: the Cu surface state at ~0.3 eV binding energy and the Co-induced state at 0.51 eV binding energy. In comparison with Fig. 6, which corresponds to slightly higher coverage of 0.06 ML, these two states are farther apart in energy at the SSBZ boundary (k_x=0.22 Å^{-1}), where the minimum of the Co-induced band lies (0.68 eV binding energy) and the Cu surface state dispersed to a higher energy (~0.2 eV) and, therefore, the EDC of the SSBZ curve in Fig. 6(b) is broader compared to the corresponding SSBZ curve in Fig. 7(c). Further, note that the Co-induced-state binding energy of 0.51 eV for 0.04 ML Co coverage is less than that at the higher 0.06 ML coverage (E_B=0.68 eV), indicating that the binding energy of the Co-induced surface state is dependent on the Co surface concentration. For the case of the terrace-normal curve in Fig. 7(c), for which the dispersion curves of the two states are within ~0.1 eV and are thus not resolved in the EDC, the total width of the terrace-normal EDC is less compared to that of the SSBZ EDC. This observation is consistent with that of Fig. 6, where the two states are closer in energy at the terrace normal than at the SSBZ boundary. At higher emission angles, the EDCs of Figs. 7(a) and 7(b) have nearly equal widths. Because of the proximity of the two bands at this coverage, the effective masses cannot be determined accurately. However, since the peak width in Fig. 7(b) decreases for larger emission angles along the steps, one can conclude that the new surface state disperses faster as it does in the case of the dispersion across the steps.

SUMMARY

To summarize, we have measured the variation of electronic structure of adsorbed layers of Co on a Cu(775) (stepped) surface with coverage of deposited Co. These measurements are thus our first step in realizing our eventual goal to relate the measured dispersion to the coverage-dependent surface structure in the bimetallic Co/Cu(775) surface system. To this end, STM studies to determine surface structure versus Co coverage are under way. The presence of the surface steps is important for two reasons: (a) they influence the surface electronic structure via a nanoscale surface periodicity and (b) they modify the growth and islanding from that on the flat surface. For the bare Cu surface, we observe a superlattice umklapp band of the surface state. We have determined that the reference plane or the position of the band minimum of this state shifts with the addition of a small amount of cobalt. We attribute this behavior to roughening of the step edges as a result of the cobalt deposition. At a sufficiently small Co coverage, we have observed the simultaneous existence of the usual Cu and a new Co-modified surface state having band minimum binding energies of ~0.3 and ~0.68 eV, respectively. These two band minima occur at parallel momenta $k_\parallel$ ~ 0.34 and ~0.22 Å^{-1}, corresponding to emission along the terrace-normal and surface-superlattice Brillouin-zone reference planes, respectively. Both of these two states disperse at approximately the same rate as the Cu(111) surface state. This new state is explained in terms of a quantum-well state hybridization with the Cu substrate

ACKNOWLEDGMENTS

*Present address: Department of Physics, Renmin University of China, Beijing, 100872, China.

[1] F. Schiller, M. Ruiz-Osés, J. Cordón, and J. E. Ortega, Phys. Rev. Lett. **95**, 066805 (2005).

[2] F. Baumberger, M. Hengsberger, M. Muntwiler, M. Shi, J. Krempasky, L. Patthey, J. Osterwalder, and T. Greber, Phys. Rev. Lett. **92**, 196805 (2004).

[3] J. Lobo, E. G. Michel, A. R. Bachmann, S. Speller, J. Kuntze, and J. E. Ortega, Phys. Rev. Lett. **93**, 137602 (2004).

[4] M. Roth, M. Pickel, W. Jinxiong, M. Weinelt, and T. Fauster, Phys. Rev. Lett. **88**, 096802 (2002).

[5] X. Y. Wang, X. J. Shen, and R. M. Osgood, Jr., Phys. Rev. B **56**, 7665 (1997).

[6] F. Baumberger, M. Hengsberger, M. Muntwiler, M. Shi, J. Krempasky, L. Patthey, J. Osterwalder, and T. Greber, Phys. Rev. Lett. **92**, 016803 (2004).

[7] J. E. Ortega, M. Ruiz-Osés, J. Cordón, A. Mugarza, J. Kuntze, and F. Schiller, New J. Phys. **7**, 101 (2005).

[8] F. Baumberger, T. Greber, and J. Osterwalder, Phys. Rev. B **64**, 195411 (2001).

[9] J. E. Ortega, A. Mugarza, A. Närmann, A. Rubio, S. Speller, A. R. Bachmann, J. Lobo, E. G. Michel, and F. J. Himpsel, Surf. Sci. **482-485**, 764 (2001).

[10] A. P. Shapiro, T. Miller, and T.-C. Chiang, Phys. Rev. B **38**, 1779 (1988).

[11] O. Sánchez, J. M. García, P. Segovia, J. Alvarez, A. L. Vázquez de Parga, J. E. Ortega, M. Prietsch, and R. Miranda, Phys. Rev. B **52**, 7894 (1995).

[12] J. E. Ortega, S. Speller, A. R. Bachmann, A. Mascaraque, E. G. Michel, A. Närmann, A. Mugarza, A. Rubio, and F. J. Himpsel, Phys. Rev. Lett. **84**, 6110 (2000).

[13] J. Lobo, E. G. Michel, A. R. Bachmann, S. Speller, L. Roca, J. Kuntze, and J. E. Ortega, J. Vac. Sci. Technol. A **21**, 1194 (2003).

[14] S. G. Louie, P. Thiry, R. Pinchaux, Y. Petroff, D. Chandesris, and J. Lecante, Phys. Rev. Lett. **44**, 549 (1980).

[15] X. J. Shen, H. Kwak, D. Mocuta, A. M. Radojevic, S. Smadici, and R. M. Osgood, Jr., Phys. Rev. B **63**, 165403 (2001).

[16] J. E. Ortega, F. J. Himpsel, R. Haight, and D. R. Peale, Phys. Rev. B **49**, 13859 (1994).

[17] H. Namba, N. Nakanishi, T. Yamaguchi, and H. Kuroda, Phys. Rev. Lett. **71**, 4027 (1993).

[18] P. Gambardella, M. Blanc, H. Brune, K. Kuhnke, and K. Kern, Phys. Rev. B **61**, 2254 (2000).

[19] A. Dallmeyer, C. Carbone, W. Eberhardt, C. Pampuch, O. Rader, W. Gudat, P. Gambardella, and K. Kern, Phys. Rev. B **61**, R5133 (2000).

[20] J. de la Figuera, J. E. Prieto, C. Ocal, and R. Miranda, Phys. Rev. B **47**, 13043 (1993).

[21] L. Diekhöner, M. A. Schneider, A. N. Baranov, V. S. Stepanyuk, P. Bruno, and K. Kern, Phys. Rev. Lett. **90**, 236801 (2003).

[22] J. de la Figuera, M. A. Huerta-Garnica, J. E. Prieto, C. Ocal, and R. Miranda, Appl. Phys. Lett. **66**, 1006 (1995).

[23] S. Speller, S. Degroote, J. Dekoster, G. Langouche, J. E. Ortega, and A. Närmann, Surf. Sci. **405**, L542 (1998).

[24] H. W. Chang, F. T. Yuan, Y. D. Yao, W. Y. Cheng, W. B. Su, C. S. Chang, C. W. Lee, and W. C. Cheng, J. Appl. Phys. **100**, 084304 (2006).

[25] J. de la Figuera, J. E. Prieto, C. Ocal, and R. Miranda, Surf. Sci. **307-309**, 538 (1994).

[26] U. Alkemper, C. Carbone, E. Vescovo, W. Eberhardt, O. Rader, and W. Gudat, Phys. Rev. B **50**, 17496 (1994).

[27] R. Miranda, F. Ynduráin, D. Chandesris, J. Lecante, and Y. Petroff, Phys. Rev. B **25**, 527 (1982).

[28] G. J. Mankey, R. F. Willis, and F. J. Himpsel, Phys. Rev. B **47**, 190 (1993).

[29] K. Ogawa, K. Nakanishi, and H. Namba, Surf. Sci. **566-568**, 406 (2004).

[30] R. H. Victora and L. M. Falicov, Phys. Rev. B **28**, 5232 (1983).

[31] F. Reinert, G. Nicolay, S. Schmidt, D. Ehm, and S. Hüfner, Phys. Rev. B **63**, 115415 (2001).

[32] M. Ø. Pedersen, I. A. Bönicke, E. Lægsgaard, I. Stensgaard, A. Ruban, J. K. Nørskov, and F. Besenbacher, Surf. Sci. **387**, 86 (1997).

[33] A. K. Schmid and J. Kirschner, Ultramicroscopy **42-44**, 483 (1992).

[34] Y. Mo, K. Varga, E. Kaxiras, and Z. Zhang, Phys. Rev. Lett. **94**, 155503 (2005).

[35] F. Reinert, B. Eltner, G. Nicolay, F. Forster, S. Schmidt, and S. Hüfner, Physica B **351**, 229 (2004).

[36] Y. W. Mo and F. J. Himpsel, Phys. Rev. B **50**, 7868 (1994).

[37] E. Bertel, Surf. Sci. **331-333**, 1136 (1995).

[38] F. J. Himpsel and D. E. Eastman, Phys. Rev. B **21**, 3207 (1980).

[39] P. D. Johnson, K. Garrison, Q. Dong, N. V. Smith, D. Li, J. Mattson, J. Pearson, and S. D. Bader, Phys. Rev. B **50**, 8954 (1994).

[40] F. Baumberger, T. Greber, B. Delley, and J. Osterwalder, Phys. Rev. Lett. **88**, 237601 (2002).